PERFORMANCE ANALYSIS AND MULTI-OBJECTIVE OPTIMIZATION OF ORIFICE PLATE MECHANICAL STRUCTURE IN AUTOMATION TRAINING

*Lele Qi, Pan Guo**
School of Mechanical and Electrical Engineering, Tangshan Maritime Institute, Tangshan, 063200, China

Abstract - In automation training, the mechanical structural performance of orifice plates has a direct correlation with the stability and efficiency of the entire automation system. However, with the ongoing advancement of automation technology, the mechanical structure of orifice plates faces various challenges, such as unstable motion, abnormal noise, vibration, etc. Therefore, the performance requirements for orifice plate mechanical structures are also increasing. In order to achieve performance analysis and multi-objective optimization of orifice plate mechanical structure, a fast non-dominated multi-objective optimization algorithm with elite retention strategy is proposed for multi-objective optimization of orifice plate mechanical transmission structure. The results show that the displacement, acceleration, velocity, and jump of the orifice plate cam under the cycloid and combined cycloid modes indicate that the dimensionless velocity and displacement curves have a smooth trend. The velocity and displacement of the combined cycloid are lower than those of the single cycloid, indicating that the combined cycloid is more compatible and applicable. The range of changes in acceleration and jump of the orifice plate mechanical structure under the combined cycloid is reduced. After optimizing the dimensionless acceleration, there is a certain decrease, from 6 to around 5 at a dimensionless time of 0.2, and the dimensionless jumps almost overlap, indicating that the mechanical properties of the orifice cam curve are improved after modulation optimization. The maximum cam pressure angle before and after optimization decreases from 43.26° to 38.59°, and the cam pressure angle during other time periods also decreases. The minimum connecting rod rotation angle increases from 86.78° to 87.5° before and after optimization, indicating that the connecting rod performance is improved. The research method significantly improves the performance of the orifice plate mechanical structure, providing better support for automation training.

Keywords: Automation training; Orifice plate motion machinery; Multi-objective optimization; NSGA-II; Genetic algorithm.

1. Introduction

In automation systems, Orifice Plates (OPs), as a common mechanical structure, are widely used in fields such as flow measurement and pressure control. The performance of OPs has a direct impact on the stability and efficiency of the whole system [1]. Therefore, in-depth analysis of the mechanical structural performance of OPs and exploration of multi-objective optimization (MOO) methods are of great significance for enhancing the overall performance of automation systems. There has been some progress in the analysis of mechanical structural performance of OPs in existing research. Single Orifice Plates (SOPs) are commonly applied in pipeline systems of nuclear power plants for throttling and depressurization of fluids in pipelines [2-3]. The cavitation caused by a SOP may lead to severe vibration of the pipeline. In order to determine the best design for a SOP with the possibility of weak cavitation, Zhang et al. modeled a novel SOP with convergent and divergent holes, proposed an MOO approach to improve the shape of the SOP, and used computational fluid dynamics to acquire fluid-related physical parameters. The mutual cavitation number and development integral are considered as the cavitation index. The outcomes revealed that the convergence angle of a SOP played a dominant role in the cavitation behavior [4]. Multi-level orifices are utilized across various industries, including oil refineries, nuclear power stations, fertilizer manufacturing facilities, and chemical

https://doi.org/10.17683/ijomam/issue22.v2.4

plants, for the purpose of pressure relief. This pressure reduction often triggers steam explosion within liquid water, giving rise to cavitation. Cavitation poses numerous challenges, such as decreased efficiency, material erosion, vibrations, and noise generation. To alleviate the adverse effects of cavitation on the system, a comprehensive understanding of the underlying phenomena is essential. Ahmed et al. proposed an improved industrial multi-stage orifice design to suppress cavitation. The true 3D setting of a six-stage orifice was simulated through Computational Fluid Dynamics (CFD) analysis. The results showed that the porous geometry with four holes on the OP exhibited the best performance under the same operating conditions, without cavitation effect [5]. The research mainly focused on porous OPs, which had superior flow measurement characteristics compared to traditional OPs. However, there was little literature on quantitative parameter research. Raheem et al. evaluated the performance of porous plates under different parameters and found that the Equivalent Diameter Ratio (EDR) had the greatest impact on the pressure loss coefficient, followed by the number of pores and compaction ratio. Under the same EDR, the pressure loss of single and porous OPs was similar, but the flow rate of porous OPs developed faster and the flow coefficient was higher. The expansion length affected the accuracy of the orifice flowmeter, but the upstream disturbance effect of the porous OP was weakened when the two-dimensional upstream length was reached. The optimal OP was selected to achieve the minimum pressure loss [6]. Compared with traditional SOPs, porous plates as throttling elements have reduced pressure drop, minimized flow-generated noise, and consistent pressure differential behavior, which is beneficial in moisture measurement. Ma et al. conducted experiments on the moisture pressure drop of two types of porous plates in stratified and intermittent flow zones in a horizontal pipeline. As the flow pattern changed, Phi (G) significantly increased. Research found that no model could accurately predict two low gas phase Froude number subregions. A new modified model combining gas phase and liquid phase Froude numbers was proposed. In the transition zone and stratified flow zone, the improved Murdoch model had the best prediction accuracy, with 15% and 6%, respectively. This helped to understand the application and prediction of porous plates in moisture measurement [7].

In recent years, the occurrence of storm geyser events has garnered considerable interest. Prior research has indicated that the employment of OPs can diminish the severity of these events. However, they may also induce pressure surges akin to water hammer on the OPs. Qian et al. created a novel simulation model for the rise of water column driven by air pockets above the OP in a vertical riser. The model considered the mass loss caused by membrane flow and OP, accurately simulating water column dynamics. Research found that initial water column length, driving pressure, and riser material significantly affected peak pressure, while riser diameter and height had a smaller impact. When the opening of the orifice was about 0.2 times the diameter of the riser, the peak pressure was at its maximum [8]. Guo et al. used a self-developed circular porous plate hydraulic cavitation device with different geometric parameters to measure the turbulent characteristics of cavitation flow behind the porous plate using Particle Image Velocimetry (PIV) technology. The experimental results showed that a high-speed multi cavitation jet was generated after the porous plate, and the flow field had a topological structure with similar longitudinal and vertical turbulence intensity. The Reynolds stress rose with the rise of the amount of holes [9]. Mechanical Choke Orifice Plate (MCOP) is a novel pattern of flow control device that can achieve throttling circumstances for incompressible fluids experiencing comparatively minor pressure reductions. Since there was a scarcity of pertinent results and data in existing literature, Liu M et al. conducted experimental research to ascertain the flow coefficient of the annular orifice, the pressure distribution within the MCOP, and the intrinsic features of the blocking flow. Their experimental findings substantiated that factors such as the Reynolds number, OP thickness, plug cone shape, and eccentricity exerted a notable influence on the aforementioned flow coefficient. Additionally, the blocking flow in MCOP could be modulated by substituting the spring, achieving a maximum flow control deviation of 4.91% [10]. Oshio et al. measured the surface temperature of a 2DOP with a 20-a-grade LaB6 hollow cathode using a near-infrared dual color radiation thermometer. The thermometer technology solved the problem of OP temperature with an accuracy of about 166 ℃, and discussed the relationship between the operating characteristics of hollow cathodes and the average surface temperature. Data analysis showed that the OP temperature displayed limited sensitivity to mass flow rate, but exhibited responsiveness to discharge current. In high current and low voltage mode, the temperature of the OP was higher, indicating higher heating efficiency of the emitter [11].

In the existing research on multi-objective optimization, the single orifice plate cavitation optimization method proposed by Zhang et al. [4] obtains fluid physical parameters (cavitation number, development integral, etc.) through CFD. Although it can reduce cavitation phenomena, it only focuses on fluid mechanics performance, does not consider the coupling effect between mechanical transmission structure parameters, and does not

involve motion stability optimization. Its applicability is limited to single orifice plate throttling and pressure reduction scenarios; The industrial multi-stage orifice plate design by Ahmed et al. [5] relies on 3D CFD simulation data to optimize the porous geometry structure, effectively suppressing efficiency degradation and vibration problems caused by cavitation. However, it does not comprehensively consider kinematic indicators such as acceleration and jump, and the optimization objective is single, lacking multi-dimensional collaborative design; Liu et al. [10] studied the flow coefficient of mechanical orifice plates and obtained pressure distribution and blockage flow characteristic data through experiments. However, their method did not construct a multi-objective optimization framework and only focused on flow control accuracy, without involving dynamic performance optimization of transmission structures. In summary, the common shortcomings of existing methods lie in their focus on a single performance indicator (cavitation, pressure loss, flow coefficient), lack of collaborative consideration of multiple objectives such as motion stability, transmission efficiency, and structural reliability, and the absence of a systematic optimization plan for orifice plate mechanical transmission structures. Relevant research data is mostly limited to fluid simulation or single performance experimental data, and fails to cover multidimensional parameters of mechanical structure kinematics and dynamics.

In summary, researchers have conducted some research on the mechanical optimization of OPs, including SOPs, cavitation index, industrial multi-stage orifice design, porous plates, and cavitation flow behind porous plates. However, the utilization of MOO algorithms to improve the transmission structure of OPs is not deep enough. In order to improve the transmission structure of OPs, an MOO algorithm-based performance optimization method for OP mechanical structures is proposed. This method innovatively analyzes the performance of OP machinery, evaluates and optimizes the cam curve, and conducts optimization research on its transmission structure, providing a technical foundation for the optimization of OP mechanical structures in automation training.

The core objective of the research is to propose an NSGA-II multi-objective optimization algorithm based on the elite retention strategy. This algorithm aims to address the issues of motion instability, vibration, noise, and insufficient transmission efficiency in the mechanical structure of orifice plates during automated training. Through the modulation optimization of cam curves and coordinated adjustment of transmission structure parameters, it achieves multi-objective improvement in the motion stability, dynamic performance, and transmission reliability of orifice plate machinery, providing technical support for the stable operation of automated training systems.

The article structure of this study is as follows: the first section focuses on the process of the MOO algorithm based mechanical structure performance optimization method for OPs designed in this study. This section represents the core and novel contribution of our research. The subsequent section delves into the experimental validation and analysis of data outcomes, grounded on the algorithm formulated in the preceding section. The final section summarizes the experimental findings, discusses the limitations of the current design, and outlines potential areas for future exploration.

2. Methods and Materials

An MOO algorithm-based method for optimizing the mechanical structure performance of OPs is proposed. Firstly, the mechanical structure performance analysis and cam curve evaluation optimization of OPs are carried out. Secondly, the fast Non-dominated Sorting Genetic Algorithm-II (NSGA-II) with elite retention strategy is combined to perform MOO design on the mechanical structure of OP transmission.

2.1 Performance Analysis of OP Mechanical Structure and Optimization of Cam Curve Evaluation

In automation training, OPs, as a common fluid control component, play an important role in automation training systems. Taking the knotting machine as an example, the OP machine is one of the key components for achieving wire knotting [12]. It completes the interweaving and knotting of meridians and parallels through the coordinated movement of upper and lower hooks, as shown in Figure 1. Therefore, when designing OP machinery, it is necessary to clarify its motion laws and coordination relationships to ensure the accuracy and stability of the knotting action.

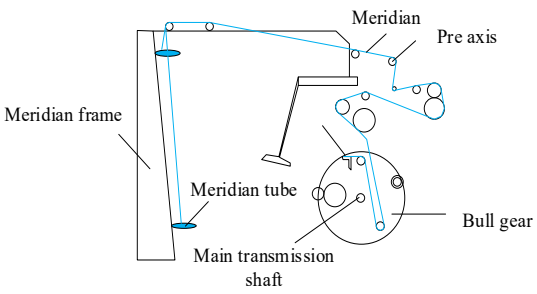

Figure 1: Structure of woven mesh machine with knots

In the study of the mechanical structural performance of OPs, computer simulation methods are employed for modeling and assessing the

kinematic performance of OPs, combined with a top-down approach to design OP structural models. The general design steps for the mechanical structure of OPs are as follows. Firstly, it is the structural layout. Based on the working principle and performance requirements, the overall layout of the OP machinery and the positional relationship of each component are determined, including the shape, size, and connection method with other components of the OP [13]. Next is material selection, selecting suitable materials based on the working environment and load requirements. OP machinery usually needs to withstand certain pressure and friction, so the material should have good mechanical properties and wear resistance. Finally, the manufacturing process takes into account the manufacturability of OP machinery to ensure that the design can be smoothly transformed into actual products, including considerations of processing methods, assembly processes, and inspection standards [14]. The collaborative design process proposed in the study is shown in Figure 2.

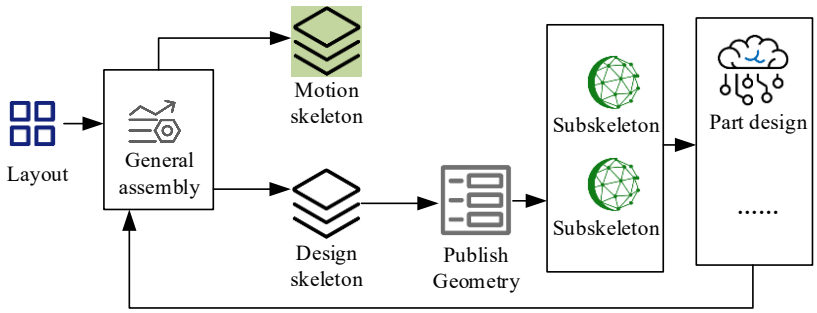

Figure 2: Collaborative design process

The cam curve is an important parameter for describing the motion law of cam mechanical followers, and its optimization holds significant importance for enhancing the kinematic and dynamic performance of machinery [15]. For the evaluation and optimization of cam curves, the first focus is on kinematic performance, as the shape of the cam curve directly affects parameters such as the speed and acceleration of the driven component. By optimizing the shape of the cam curve, smooth motion of the driven component can be achieved, reducing vibration and impact, and improving the precision and stability of mechanical motion. Next is the dynamic performance, and optimizing the cam curve can also improve the mechanical dynamic performance. Finally, the feasibility and cost of machining need to be considered when optimizing the cam curve. Overly complex cam curves may increase machining difficulty and cost, so it is necessary to choose simple and easy to machine cam curve shapes while meeting performance requirements [16].

In the knotting machine, the OP movement mechanism drives the OP to perform composite motion through a cam mechanism, completing the knotting action of the wire mesh. At this point, the shape of the cam curve will directly affect the motion and performance of the OP. Therefore, when conducting performance analysis of OP mechanical structure and optimization of cam curve evaluation, it is necessary to comprehensively consider these two factors in order to achieve overall performance optimization of the system. Firstly, the cam curve is dimensionless, including motion characteristics such as constant velocity, equal acceleration, equal deceleration, negative equal step, positive equal step, cosine acceleration, and double harmonic. The study selected features such as sine corrected constant velocity, trapezoidal acceleration, corrected trapezoidal acceleration, and combined cycloid, and expressed these cam curves and influencing factors as shown in equation (1).

$$A=\{a_1,a_2,a_3,a_4\}=\{V_m,A_m,J_m,T_m\} \tag{1}$$

In equation (1), a_1, a_2, a_3, and a_4 represent features. V_m, A_m, J_m, and T_m represent factors influencing features. Then, based on fuzzy comprehensive evaluation, the cam curve is evaluated and a membership matrix is constructed, as shown in equation (2).

$$R=\left(r_{ij}\right)_{n\times m} \tag{2}$$

In equation (2), R is the membership matrix and r_{ij} is the matrix elements. The calculation of the corresponding judgment matrix elements is shown in equation (3).

$$r_{ij}=1-\frac{x_{ij}}{x_{ij}^{UP}+x_{ij}^{DOWN}} \tag{3}$$

In equation (3), x_{ij} represents the various eigenvalues of the Tern curve, x_{ij}^{UP} represents the maximum eigenvalue of the target i, and x_{ij}^{DOWN}

represents the minimum eigenvalue of the target i .After using expert weighting method to determine the factor weights of feature values, the fuzzy subset for comprehensive evaluation judgment is calculated and expressed as equation (4).

$$B = W \cdot R = \left(b_1, b_2, \cdots, b_n\right) \tag{4}$$

In equation (4), R represents the fuzzy subset of comprehensive evaluation judgment, $\cdot$ represents the matrix operator, and W represents the weight coefficient vector. After evaluating the mechanical cam curve of the OP above, the study aims to optimize the amplitude modulation of the mechanical cam curve for OP motion. The basic principle of amplitude modulation optimization is to generate a new curve expression to display excellent motion or dynamic performance, with a fuller curve and smaller peak eigenvalues. By amplitude modulation optimization, the motion characteristics of the cam curve can be improved, the impact and vibration of the driven component during motion can be reduced, and the smoothness and reliability of the mechanical system can be improved. Meanwhile, by optimizing the cam curve, the inertia force and vibration of the driven components can be reduced, thereby improving the dynamic performance and stability of the mechanical system.

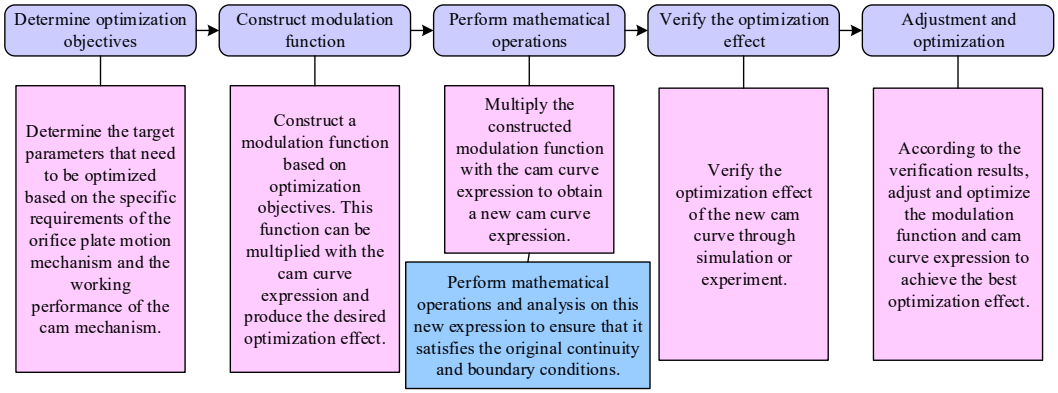

Figure 3: Implementation steps for amplitude modulation optimization

In Figure 3, based on the specific requirements of the OP motion machinery and the working performance of the cam machinery, the target parameters that need to be optimized are determined, such as the maximum speed and maximum acceleration. A suitable modulation function is constructed based on optimization objectives. This function should be able to multiply with the cam curve expression and produce the desired optimization effect. Finally, a new expression for the cam curve is obtained. Then, the system performs mathematical operations and analysis on this new expression to ensure that it satisfies the original continuity and boundary conditions. It verifies the optimization effect of the new cam curve through simulation or experiment. This includes checking the motion accuracy, smoothness, and dynamic performance of the mechanical system of the driven components. According to the verification results, adjust and optimize the modulation function and cam curve expression to achieve the best optimization effect.

2.2 MOO Design of Mechanical Transmission Performance for OP Motion

With the continuous development of intelligent and digital technology, the performance analysis and MOO research of OP mechanical structures will pay more attention to technological integration and innovation. Optimization methods can be used to improve the problems with cam curves, such as motion performance fluctuations caused by irregularities. The study adopts MOO methods to improve the mechanical transmission performance of OP motion. Firstly, an MOO model is constructed. The multi-objective optimization criteria studied include three interrelated core dimensions: minimizing the maximum pressure angle of the cam (α_{max}), reducing the impact between the cam and the follower, and improving the smoothness of motion; Maximizing the minimum rotation angle of the connecting rod (γ_{min}): enhancing the transmission efficiency of the connecting rod and avoiding sticking phenomenon; Minimize the maximum angular acceleration of the swing arm (β_{max}): reduce vibration and noise, and improve structural reliability. $f(x)$ expresses the overall optimization objective as shown in equation (5).

$$\begin{aligned} &min\, f(x) = \left[f_1(x), f_2(x), f_3(x)\right] \\ &s.t. \\ &h_i(x) \le 0 \left(i = 1, 2, ..., k\right) \\ &g_i(x) = 0 \left(j = 1, 2, ..., h\right) \\ &x \in \left[x_{min},\ x_{max}\right] \end{aligned} \tag{5}$$

In equation (5), $f_1(x)=\alpha_{max}$ represents the maximum pressure angle of the cam and the target is minimized; $f_2(x)=-\gamma_{min}$ represents the minimum rotation angle of the connecting rod, maximizing the target is equivalent to minimizing its negative value; $f_3(x)=\beta_{max}$ represents the maximum angular acceleration of the swinging arm, minimizing the target; $x=[l_3,\ l_4,\ \psi_0]$ represents the design variable, l_3 is the distance between the boom roller and the swing center, l_4 is the variable rod length, and ψ_0 is the initial swing angle of the swing arm; $h_i(x)$ is an inequality constraint: α_{max} ≤ 40 °, $-\gamma_{min}$ ≥ 85 °; $g_i(x)$ is an equality constraint: satisfies the geometric motion relationship of the cam link combination mechanism; $[x_{min},\ x_{max}]$ is the range of values for the design variable. OP motion machinery is one of the main components of a woven mesh machine, and its performance directly affects the overall performance of the machine and the quality of the finished products with woven mesh. Therefore, optimizing the mechanical transmission performance of OP motion is of great significance, and the research adopts NSGA-II for MOO improvement. NSGA-II, as a popular MOO genetic algorithm, has the advantages of fast running speed and good solution convergence, and is suitable for performance optimization of such complex mechanical systems [17].

The conceptual flowchart of the proposed Multi Objective Optimization (MOO) method is shown in Figure 4.

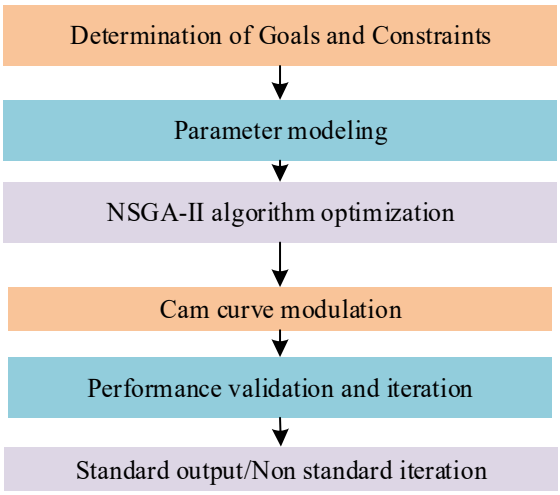

Figure 4: Conceptual flowchart of multi-objective optimization (MOO) method proposed

In Figure 4, firstly, based on the work requirements of orifice plate machinery in automated training, the optimization objectives are clearly defined, and constraints are set; Secondly, design variables and construct a multi-objective optimization mathematical model; Subsequently, the NSGA-II algorithm is used to complete population initialization, non dominated sorting, crowding calculation, and selection/crossover/mutation operations, generating Pareto optimal solutions; Next, based on the optimal solution, amplitude modulation is applied to the cam curve to generate a new curve that meets the requirements of motion smoothness; Finally, the kinematic and dynamic performance of the optimized structure is verified through numerical simulation. If the preset indicators are not met, the parameter modeling stage is returned to adjust the constraints or target weights until the optimal solution is obtained.

The NSGA-II algorithm with elite retention strategy is selected for multi-objective optimization of orifice plate mechanical transmission structure. The following argument is presented. The mechanical optimization of orifice plates requires the simultaneous achievement of three major objectives: minimizing the maximum pressure angle of the cam, maximizing the minimum rotation angle of the connecting rod, and minimizing the maximum angular acceleration of the swing arm. These objectives conflict with each other (such as reducing the pressure angle which may lead to insufficient rotation angle). However, the non dominated sorting mechanism and elite retention strategy of NSGA-II can efficiently generate a uniformly distributed Pareto optimal solution set, meeting the requirements of multi-objective collaborative optimization; Compared with traditional genetic algorithms, NSGA-II avoids local optima through crowding degree calculation and adapts to the characteristics of orifice plate machinery, such as "multiple design variables (swing arm length, initial angle, etc.) and complex constraint conditions (pressure angle range, transmission angle lower limit)", which can improve the diversity and global optimality of optimization solutions; This algorithm has fast running speed, good convergence, and can quickly handle the computational complexity caused by the coupling of mechanical structural parameters. It meets the dual requirements of optimization efficiency and accuracy for automated training equipment and provides efficient and reliable technical support for subsequent experimental verification.

The main drive shaft is the core component of OP motion machinery, which transmits power through rotation and drives the OP to perform various movements [18]. In equipment such as weaving machines, the spindle is usually coordinated with components such as motors, pulleys, and gears to achieve power transmission and conversion. Its mechanical model is shown in Figure 5.

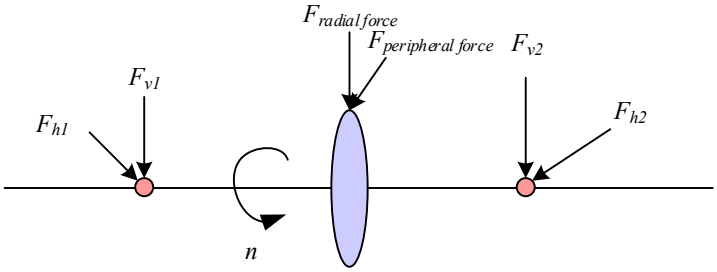

Figure 5: Simplified mechanical model of main drive shaft

In Figure 5, Fv1 and Fv2 represent vertical downward forces, $F_{radial\ force}$ is radial force, and $F_{peripheral\ force}$ is peripheral force. Fh1 and Fh2 represent oblique downward forces and n is spindle speeds. When transmitted to the gear, the torque calculation is shown in equation (6).

$$Torque = 9.66 \times 10^3 \times P\eta / n \tag{6}$$

In equation (6), P represents motor power, η represents transmission efficiency to the large gear, and $Torque$ represents torque. The peripheral force calculation is shown in equation (7).

$$F_{peripheral\ force} = 2Torque / d \tag{7}$$

In equation (7), d represents the diameter of the large gear indexing circle and α represents the gear pressure angle. The calculation of radial force is shown in equation (8).

$$F_{radial\ force} = F_{peripheral\ force} \times \tan\alpha \tag{8}$$

The calculation of bearing stiffness is shown in equation (9).

$$G = 1.7826488 \times 10^7 \frac{\cos^2\alpha}{\sqrt[3]{\sin\alpha}} \times \sqrt[3]{f_0} \times \sqrt[3]{Z_n{}^2 D_g} \tag{9}$$

In equation (9), Z_n represents the number of rolling elements in the bearing, f_0 represents the preload force of the bearing, G represents the stiffness of the bearing, and D_g represents the diameter of the rolling elements in the bearing. The motion performance of the main drive shaft can be analyzed as shown in Figure 6.

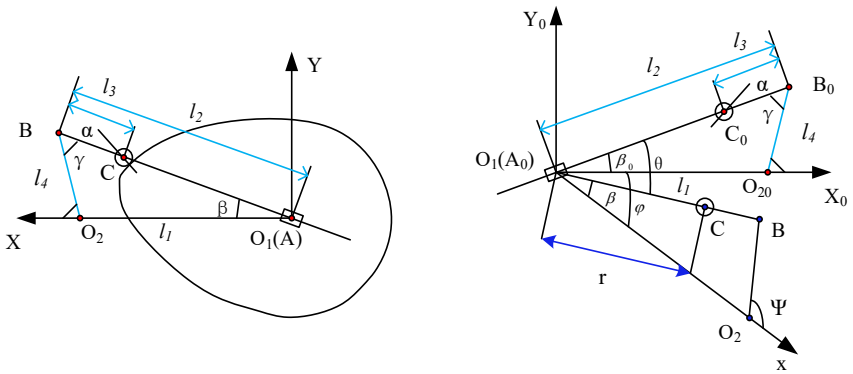

Figure 6: Schematic diagram of cam theoretical profile for the combination mechanism of upper and lower cam links on the OP and the reverse method: a-Combination mechanism of upper and lower cam linkage on orifice plate; b-Reverse method diagram of cam theoretical contour

In Figure 6, the up and down movement of the OP is usually achieved by a cam linkage combination mechanism. This type of machinery consists of components such as a cam, connecting rod, and swing arm. The rotation of the cam drives the movement of the connecting rod and swing arm, thereby achieving the up and down movement of the OP [19]. The reversal method is a technique used for designing cam profile curves, based on the principle of relative motion invariance [20-21]. The transmission performance of the mechanical structure of the OP is analyzed using the reverse method for illustration. The calculation of the mechanical pressure angle of the cam connecting rod is shown in equation (10).

$$\alpha = \arctan\frac{dr}{r \times d\theta} \tag{10}$$

In equation (10), the polar coordinate form of the origin of the coordinate system is (r,θ), and θ represents the rotation angle. By analogy, the cam

rotation angle, connecting rod rotation angle, etc. are obtained, as shown in equation (11).

$$\begin{cases} \begin{cases} x_b = l_4 \cos\psi + l_1 \\ y_b = l_4 \sin\psi \end{cases} \\ r = l_2 - l_3, l_2 = \sqrt{x_b^2 + y_b^2} \end{cases} \tag{11}$$

In equation (11), ψ represents the variable of the angle between the x-axis of the coordinate system and the joystick l_4, l_2 and l_3 represent the length of the variable rod, and $\sqrt{x_b^2 + y_b^2}$ represents the length of the variable rod in the B coordinate. Then a mathematical model for optimizing the mechanical structure of the OP is constructed, with the objective function shown in equation (12).

$$\min f_1(x) = \alpha_{\max}, \min f_2(x) = -\gamma_{\min} \tag{12}$$

In equation (12), $\alpha_{\max}$ represents the maximum concave wheel pressure angle and $\gamma_{\min}$ represents the minimum connecting rod rotation angle. Then, variables are designed and selected for the study, including the initial rotation angle of the swing arm, the length of the swing arm, and the distance between the large arm roller and the swing center, as expressed in equation (13).

$$x = [x_1, x_2, x_3] = [l_3, l_4, \psi_0] \tag{13}$$

In equation (13), l_3 represents the distance between the arm roller and the swing center, l_4 represents the length of the swing arm, and ψ_0 represents the initial rotation angle of the swing arm. Constraint $E_1(x), E_2(x)$ is set and the pressure angle range of the camshaft is shown in equation (14).

$$E_1(x) = \alpha_{\max} - [\alpha], 0 \tag{14}$$

In equation (14), $[\alpha]$ represents the allowable pressure angle value. For the swing angle of the groove type cam, the constraint is shown in equation (15).

$$E_2(x) = [\gamma] - \gamma_{\min}, 0 \tag{15}$$

In equation (15), $[\gamma]$ represents the minimum transmission angle swing limit value. Then MOO is performed, as shown in Figure 7.

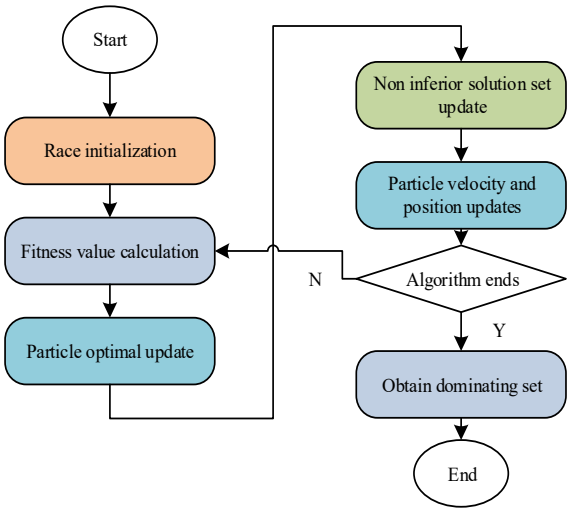

Figure 7: Optimization method for mechanical structure performance of OP based on MOO

3. Results

In order to validate the MOO based mechanical structure performance optimization method for OPs proposed in the research, an experiment was conducted to verify it, analyze the corresponding design parameters and experimental data results, verify the advantages and feasibility of the method, and provide reference for OP structure design.

3.1 MOO Experiment on Mechanical Structural Performance of OP

Numerical simulation methods were used to optimize its structural form and further study its basic energy dissipation laws. The study selected a woven mesh machine produced by a certain company and conducted MOO on its OP mechanical structure performance. The OP and MOO parameters are shown in Table 1.

Table 1 OP and MOO parameters

Design variable	x1 (mm)	x2(mm)	x3(mm)
Initial value	170	198.6	128
Parameter	Rack (mm)	Spindle speed (°/s)	/
Parameter values	550	120	/
NSGA-II parameters	NSGA-II parameter values	NSGA-II parameters	NSGA-II parameter values
Optimal front-end individual coefficient	0.2	Stop Algebra	200
Population size	200	Adaptation function value error	0.01
Maximum number of evolutions	200	/	/

Figure 8 shows the displacement, acceleration, velocity, and jump of the orifice cam under the cycloidal and combined cycloidal modes. In Figure 8 (a), the trend of dimensionless velocity and displacement curves was smooth, and the velocity and displacement of the combined cycloid were lower than those of the single cycloid, indicating that the combined cycloid was more compatible and applicable.

In Figure 8 (b), the range of acceleration and jump of the OP mechanical structure under the combined cycloid has decreased.

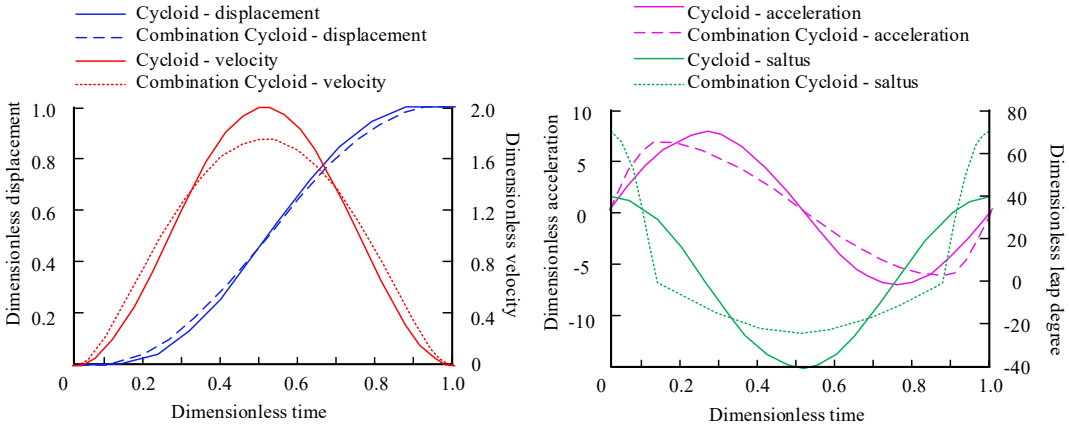

(a) Dimensionless displacement and velocity (b) Dimensionless acceleration and jump

Figure 8: Displacement, acceleration, velocity, and jump of orifice cam under cycloidal and combined cycloidal modes

Figure 9 shows the dimensionless displacement, velocity, acceleration, and jump changes of the OP mechanical structure before and after optimization. In Figure 9 (a), compared with before optimization, the dimensionless displacement almost overlapped after optimization, and there was a certain decrease after dimensionless velocity optimization. In Figure 9 (b), there was a certain decrease in the non-dimensional acceleration after optimization, from 6 to around 5 at a non-dimensional time of 0.2, while the non-dimensional jumps almost overlapped, indicating that the mechanical performance of the orifice cam curve was improved after modulation optimization.

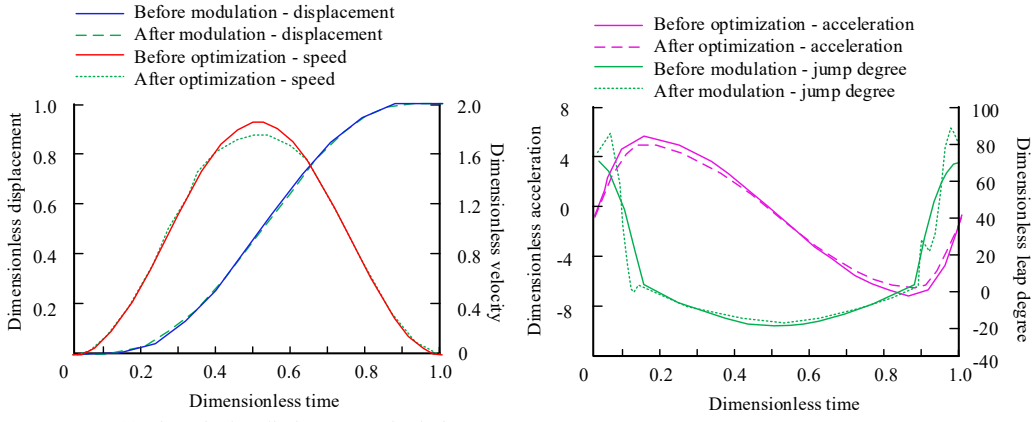

(a) Dimensionless displacement and velocity (b) Dimensionless acceleration and jump

Figure 9: Changes in displacement, velocity, acceleration, and jump of the mechanical structure of the OP before and after optimization

3.2 Analysis of Optimization Results for Mechanical Structure Performance of OP

Table 2 shows the parameter optimization of OPs before and after optimization using different methods. The experiments selected methods from references [4], [5], and [10], which were proposed by Zhang et al. as an MOO method to optimize the shape of a SOP. Optimizing the design of a SOP could reduce the downstream jet area and upstream pressure. Ahmed et al. proposed an improved industrial multi-stage orifice design to suppress cavitation. Liu et al. Proposed the improved flow coefficient and pressure distribution characteristics of the annular orifice. The selected optimization parameters for the OP were variable rod length (*l3*,*l4*) and angle variable (*PSI*). The method in reference [4] also optimized the OP, with*l3*reduced to *165mm*, *l4*reduced to *203mm*,

and *PSI* reduced to 126°. The optimization results of the method in reference [5] showed that*l3*decreased to *166mm*, *l4*increased to *209mm*, and PSI decreased to 123°. The optimization results of the method in reference [10] showed that*l3*increased to *173mm* (close to the original value), *l4*decreased to *204mm*, and *PSI* decreased to 128°. The research method was optimized for the OP, resulting in a decrease in *l3*to *161mm*, an increase in *l4* to *215mm*, and a decrease in *PSI* to 125°.This indicated that the research method achieved optimization by adjusting the variable rod length and angle variables.

Table 2 Parameter optimization of OPs before and after optimization using different methods

Method	l3 (mm)	l4 (mm)	Ψ (°)
Original unoptimized	172	198.2	130
Research method	161	215	125
Literature [4] Method	165	203	126
Literature [5] Method	166	209	123
Literature [10] Method	173	204	128

Figure 10 shows the changes in the rotation angle of the orifice cam and connecting rod before and after optimization. In Figure 10 (a), the maximum cam pressure angle before and after optimization decreased from 43.26° to 38.59°, and the cam pressure angle also decreased in other time periods, indicating an improvement in the performance of the cam. In Figure 10 (b), the minimum link rotation angle increased from 86.78° to 87.5° before and after optimization, indicating an improvement in link performance.

Figure 11 shows the swing arm angular acceleration curves of the cam before and after assembly optimization. From Figure 11 (a) - (b), the maximum angular acceleration of the swing arm before and after cam optimization was 1958.56°/s² and 1615.14°/s², respectively, a decrease of 343.42°/s². In other time periods, the overall angular acceleration of the swing arm after optimization decreased to a certain extent. The research method was effective in optimizing the structure of OP machinery.

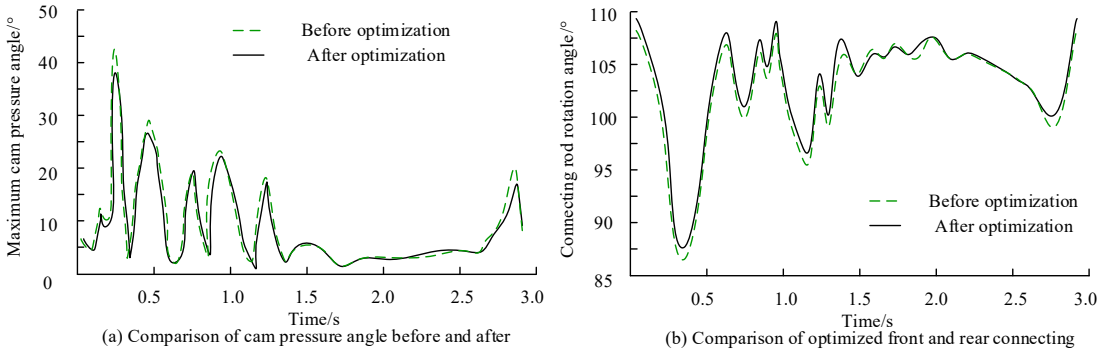

(a) Comparison of cam pressure angle before and after optimization

(b) Comparison of optimized front and rear connecting rod transmission angles

Figure 10: Changes in the rotation angle of the orifice cam and connecting rod before and after optimization

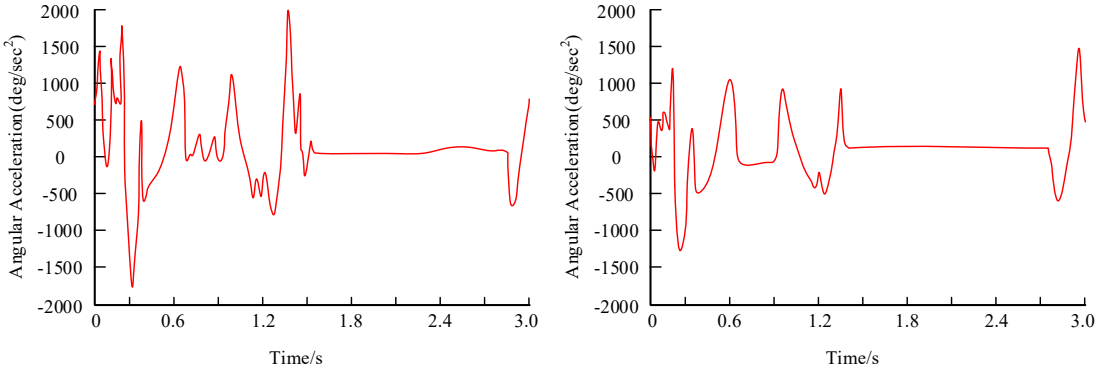

(a) Assembling the angular acceleration curve of the swing arm with the original cam

(b) The swing arm angular acceleration curve of the cam after assembly optimization

Figure 11: Swing arm angular acceleration curve of cam before and after assembly optimization

4. Conclusions

In automation training, the mechanical structure of the OP is a key component, and its performance directly affects the stability and efficiency of the entire system. The study proposed using NSGA-II for MOO, which was an effective method to improve the mechanical transmission performance of OP motion. The results showed that from the non-dimensional displacement, velocity, acceleration, and jump

changes of the OP mechanical structure before and after optimization, compared with before optimization, the non-dimensional displacement almost overlapped after optimization, while the non-dimensional velocity decreased to a certain extent after optimization. At a non-dimensional time of 0.2, it decreased from 6 to around 5, and the non-dimensional jump also almost overlapped, indicating that the mechanical performance of the OP cam curve was improved after modulation optimization. The research method was optimized for the OP, resulting in a decrease in *l3*to *161mm*, an increase in *l4*to *215mm*, and a decrease in *PSI* to 125°.The maximum cam pressure angle change before and after optimization decreased from 43.26° to 38.59°. The minimum rotation angle of the connecting rod increased from 86.78° to 87.5° before and after optimization, indicating an improvement in the performance of the connecting rod. Before and after cam optimization, the maximum angular acceleration of the swing arm decreased by 343.42°/s^2 to 1958.56°/s^2 and 1615.14°/s^2, respectively. In other time periods, the overall angular acceleration of the optimized swing arm decreased to a certain extent. The research method was effective in optimizing the structure of OP machinery. However, the application of new materials, manufacturing processes, and control technologies in OP mechanical structures increased the complexity and uncertainty of research. Therefore, in future research, it is necessary to establish unified design standards, testing methods, and evaluation indicators to help improve the universality and interchangeability of OP mechanical structures.

Acknowledgement

The research is supported by: 2024 China Jianggu Education Science Research Project: “Research on the Operation Mode of PLC Course Training” Project Number: ZGJGJYKE17; 2021 Tangshan Maritime Institute level Project: “Research on the Construction of Ideological and Political Resources in the Course of Sensor and Detection Technology” Project Number: SZ2021004.

References

[1] Mahapatra J, Tiwari P S, Singh K P, Nandede B M, Singh J, Sahni R K. Flexible orifice seed metering plate to address variability in seed shape, size and orientation enhances field performance of a pneumatic planter. Discover Applied Sciences, 2024, 6(11):1-19.

[2] Weise J, Balio J L, Paladino E E.CFD study of the transient wet gas flow behavior through orifice plate flow meters. Flow Measurement and Instrumentation, 2021, 82(1):102077.1-102077.15.

[3] Kudrna P. Effects of Orifice Plate as a Flow Sensor in an Endotracheal Tube on the Ability of Elimination CO 2 during HFJV-Animal Study Citation: Kudrna, P. Effects of Orifice Plate as a Flow Sensor in an Endotracheal Tube on the Ability of Elimination CO 2 during. Applied Sciences, 2021,11(9):4210-4211.

[4] Zhang Y, Lai J, He C, Yang S. Cavitation optimization of single-orifice plate using CFD method and neighborhood cultivation genetic algorithm. Nuclear Engineering and Technology, 2022, 54(5):1835-1844.

[5] Ahmed S A, Hassan A, Zubair R, Rashid S, Ullah A. Design modification in an industrial multistage orifice to avoid cavitation using CFD simulation. Journal of the Taiwan Institute of Chemical Engineers, 2023,148(1):104833.1-104833.10.

[6] Raheem A, Siddiqi A S B, Ibrahim A, Ullah A, Inayat M H. Evaluation of multi-holed orifice flowmeters under developing flow conditions - An experimental study. Flow Measurement and Instrumentation, 2021,79(1):1-16.

[7] Ma Y, Lyu J, Liu W. Wet gas pressure drop across multi-orifice plate in horizontal pipe in low gas-phase Froude number region. Journal of the Taiwan Institute of Chemical Engineers, 2021,127(1):92-101.

[8] Qian Y, Zhu D. Impact pressure on an orifice plate by a rising water column driven by an air pocket in a vertical riser. Water science and technology: a journal of the International Association on Water Pollution Research, 2020, 81(5):1029-1038.

[9] Guo Z P, Sun X H, Dong Z Y. PIV analysis and high-speed photographic observation of cavitating flow field behind circular multi-orifice plates. Water Science and Engineering, 2020, 13(2):145-153.

[10] Liu M, Zhang X, Wang D. Experimental Study on the Flow Characteristics of a Plate with a Mechanically Choked Orifice. Fluid Dynamics & Materials Processing, 2021,17(1):97-107.

[11] Oshio Y, Hirai K, Watanabe H, Horisawa H, Funaki I. Orifice plate surface temperature measurement of a LaB6 hollow cathode using a near-infrared two-color radiation thermometer. Journal of Electric Propulsion, 2024, 3(1):1-19.

[12] Yang B. Research on the Influence of Rectifying Orifice Plate on the Airflow Uniformity of Exhaust Hood. Applied Sciences, 2024, 14(21):9917-9918.

[13] Hai-Ji W, Guang-Lin S. Study and Design of Damping Orifice of Slipper/Swash Plate Pair. Manufacturing Automation, 2021, 45(3):148-152.

[14] Ma Y, Ma Y, Lyu J, Liu W. Experimental study on prediction model of wet gas pressure drop across single-orifice plate in horizontal pipes in the low

gas phase Froude number region. Chinese Journal of Chemical Engineering,2022,4(6):63-72.

[15] Liu J W S. Wet gas pressure drop across orifice plate in horizontal pipes in the region of flow pattern transition. Flow Measurement and Instrumentation, 2020, 71(1):101678-101679.

[16] Chen L, Ma H , Ma G , Pan G, Li P, Sun Z. Erratum to "Performance improvement prediction of push chain moist-mix concrete spraying machine employing orifice plate". Journal of Mechanical Science & Technology, 2022, 36(11):1-12.

[17] Lan T S, Chiu M C, Cheng H C, Lin Y D. Numerical Analysis of Silencers Composed of Screw Tube, Expansion Cone, Orifice Plate, and Perforated Tube by Finite Element Method. Sensors & Materials, 2024, 36(6):1-12.

[18] Vemulapalli S, Venkata S K. Parametric analysis of orifice plates on measurement of flow: A review. Ain Shams Engineering Journal, 2022, 13(3):1-6.

[19] Wen J, Tian R, Tan S, Sun Q, Gu H. The weeping characteristic of submerged multi-orifice plate - ScienceDirect. Chinese Journal of Chemical Engineering, 2020, 28(4):955-968.

[20] Prabhu V, Velnath R, Vairavel K S. Corrosion Detection of an Orifice Plate for Flow Rate Measurement using Heat Transfer Mechanism. IOP Conference Series Materials Science and Engineering, 2021, 1084(1):12065.1-12065.10.

[21] G Mehdi, H Hooman, Y Liu, S Peyman and R. Arif Data Mining Techniques for Web Mining: A Survey. Artificial Intelligence and Applications, 2022, 1(1):3-10.